

## Original Article

# Anillin contributes to prostate cancer progression through the regulation of IGF2BP1 to promote c-Myc and MAPK signaling

Jinke Liu<sup>1\*</sup>, Shiyu Wang<sup>2\*</sup>, Cong Zhang<sup>1</sup>, Ziwei Wei<sup>1</sup>, Dunsheng Han<sup>1</sup>, Yufeng Song<sup>1</sup>, Xiaoming Song<sup>1</sup>, Fan Chao<sup>3</sup>, Zhiming Wu<sup>4</sup>, Guoxiong Xu<sup>2</sup>, Gang Chen<sup>1</sup>

<sup>1</sup>Department of Urology, Jinshan Hospital, Fudan University, Shanghai 201508, China; <sup>2</sup>Research Center for Clinical Medicine, Jinshan Hospital, Fudan University, Shanghai 201508, China; <sup>3</sup>Department of Urology, Zhongshan Hospital, Fudan University (Xiamen Branch), Xiamen 361015, Fujian, China; <sup>4</sup>Department of Urology, Sun Yat-sen University Cancer Center, Guangzhou 510060, Guangdong, China. \*Equal contributors.

Received November 14, 2023; Accepted January 18, 2024; Epub February 15, 2024; Published February 28, 2024

**Abstract:** Prostate cancer (PCa), especially castration-resistant PCa, is a common and fatal disease. Anillin (ANLN) is an actin-binding protein that is involved in various malignancies, including PCa. However, the regulatory mechanism of ANLN in PCa remains unclear. Exploring the role of ANLN in PCa development and discovering novel therapeutic targets are crucial for PCa therapy. In the current work, we discovered that ANLN expression was considerably elevated in PCa tissues and cell lines when compared to nearby noncancerous prostate tissues and normal prostate epithelial cells. ANLN was associated with more advanced T stage, N stage, higher Gleason score, and prostate-specific antigen (PSA) level. In addition, we discovered that overexpression of ANLN promoted PCa cell proliferation, migration, and invasion *in vitro* and *in vivo*. Mechanistically, we performed RNA-seq to identify the regulatory influence of ANLN on the MAPK signal pathway. Furthermore, a favorable association between ANLN expression and IGF2BP1 expression was identified. The tumor-suppressive impact of ANLN downregulation on PCa cell growth was partially reversed by overexpressing IGF2BP1. Meanwhile, we discovered that ANLN can stabilize the proto-oncogene c-Myc and activate the MAPK signaling pathway through IGF2BP1. These findings indicate that ANLN could be a potential therapeutic target in PCa.

**Keywords:** ANLN, IGF2BP1, MAPK, c-Myc, proliferation, metastasis, prostate cancer

## Introduction

Prostate cancer (PCa) is one of the most prevalent malignant tumors in men. According to the American Cancer Society, there will be 288,300 new cases of PCa in 2023, accounting for 29% of all male tumors and ranking first in male tumor incidence, and 34,700 deaths from the illness, ranking second in male cancer mortality [1]. Radical surgery, radioactive seed implantation, or external radiation are currently available treatments for localized PCa, but androgen deprivation therapy is still the only option for treating advanced PCa [2]. The majority of advanced patients will develop castration-resistant PCa, which is resistant to current treatments [3]. Finding novel treatment targets and researching the molecular mechanisms

that underlie the development of PCa have therefore become crucial.

Anillin (ANLN), a gene that encodes an actin-binding protein with 1,125 amino acids, is located on chromosome 7q14.2 and is important for cytokinesis. It has a conserved N-terminal actin (F-actin) and myosin binding region as well as a conserved C-terminal pH binding domain [4-6]. ANLN expression levels were significantly raised in a range of tumor tissues, including those from breast, ovarian, colon, lung, and pancreatic malignancies [7-12]. Recent studies suggest that dysregulated ANLN plays a role in tumor initiation, growth, and development. For instance, it has been demonstrated to promote the growth of pancreatic cancer via altering the EZH2/miR-218-5p/

## Anillin promotes prostate cancer progression

LASP1 signaling axis [13]. Through the activation of RhoA, ANLN improved doxorubicin resistance in breast cancer cells [14]. ANLN plays an important function in human lung carcinogenesis by activating RhoA and participating in the phosphoinositide 3-kinase/AKT pathway [14]. Additionally, ANLN is widely expressed in PCa tissues, and its levels of expression are related to the pathogenic grade and stage of the illness. However, it is uncertain which signaling pathways and molecular targets are involved in controlling PCa development function.

IGF2BPs are made up of six standard RNA-binding domains, two recognition motifs, and four K-homology domains [15]. IGF2BP1, one of these family members, has been shown to enhance the stability of target mRNA and control gene translation via K homology domains in a m6A-dependent manner [16]. IGF2BP1 levels have been linked to the growth and metastasis of tumors in esophageal adenocarcinomas, leukemia, melanoma, osteosarcoma, rhabdomyosarcoma, and breast, liver, lung, and gastrointestinal malignancies, according to previous research [17]. They are also recognized for positively regulating the expression of a number of oncogenic factors, including KRAS, c-Myc, which promotes tumor cell growth, and MDR1, which contributes to tumor cells' drug resistance [15]. Through interactions with other proteins, IGF2BP1 is also recognized for its contribution to signal transduction pathways such PI3K, mTOR, and MAPKs [18-20]. In addition to cell proliferation, IGF2BP1 has been shown to affect tumor cell migration via MK5 and PTEN signaling [21]. However, its precise biological role in PCa is unknown.

Intracellular signaling mediated by the Erk/MAPK pathway is connected with a wide range of cellular functions, including cell proliferation, differentiation, survival, death, and transformation [22, 23]. Both primary and metastatic PCa lesions were discovered to have greatly raised MAPK levels [24] and inhibiting this pathway was proven to be very efficient at preventing the development of metastatic prostate cancer [25]. The activation of the MAPK pathway has been linked to the advancement of prostate cancer to a more advanced stage [26, 27].

Here, we found that ANLN was significantly raised in PCa tissues and highly correlated with

the prognosis of PCa patients. Additionally, we first discovered that ANLN exerts its oncogenic role in PCa cells via IGF2BP1 to activate the MAPK signal pathway and stabilize the proto-oncogene c-Myc. Our finding provided a new insight into the treatment of PCa.

### Materials and methods

#### *Patient tissue specimens and cell lines*

30 matched PCa and ANP tissues were pathologically validated by two different pathologists. This study was approved by the Ethics Committee of Jinshan Hospital, Fudan University. All patients gave their consent for the use of their specimens for scientific research.

#### *Cell lines*

FuHeng Cell Center (Shanghai, China) provided HEK293T cells, human PCa cell lines (DU145, PC-3), and human normal prostate epithelial cells (RWPE-1). HEK293T and DU145 cells were grown in DMEM (Gibco, Thermo Fisher Scientific Inc., USA). PC-3 was grown in DMEM/F12 (HyClone, GE Healthcare Life Science, Utah, USA). RWPE-1 was grown on keratinocyte SFM (Gibco, Thermo Fisher Scientific Inc., USA). All culture mediums were supplemented with 10% fetal bovine serum (FBS; BI, Beit Haemek, Israel). All cell lines were grown at 37°C with 5% CO<sub>2</sub>.

#### *RNA interference*

PC-3 and DU145 cells were grown to 60% confluence in 6-well plates at the time of transfection. Following the manufacturer's instructions, si-ANLN-1, si-ANLN-2, and negative control siRNAs (GenePharma, Shanghai, China) were transfected using X-tremeGENE siRNA Transfection Reagent (Roche, Man Manheim, Germany). Sequences of the siRNAs were listed in [Table S1](#).

#### *Plasmid vector construction and transfection*

The CDS of ANLN was synthesized and cloned into the overexpression vector copGFP-pLVX-Puro (NovoPro, Shanghai, China) for the ANLN overexpression vector. The empty vector without the ANLN insertion was used as a negative control.

## Anillin promotes prostate cancer progression

For the ANLN knocking-down vector, Sh-ANLN-1, Sh-ANLN-2, and Sh-NC were made into short hairpin RNAs, synthesized, and cloned into vector PLKO.1 (Genewiz, Suzhou, China). The sequences of sh-ANLN-1, sh-ANLN-2, and sh-NC are listed in [Table S2](#).

The LipoD293 DNA transfection reagent (SignaGene Laboratories, Rockville, USA) was used to co-transfect pMD2.G, pSPAX2, and Plvx-IRES-Puro into HEK293T cells, promoting lentivirus production. Puromycin was employed to select and maintain stable cells.

### *RNA extraction and quantitative real-time polymerase chain reaction (qRT-PCR)*

TRIzol Reagent (Takara, Shiga, Japan) was used to extract total RNA from PCa and ANP tissues. Total RNA was extracted from cell lines using the RNA-Quick Purification Kit (Yishan, Shanghai, China). Nanodrop 2000 (Thermo Fisher Scientific, Waltham, USA) was used to quantify RNA purity and concentration. PrimeScript RT Master Mix (Takara, Shiga, Japan) was used for reverse transcription. A qRT-PCR reaction system was prepared using the BeyoFast SYBR Green qPCR Mix (Beyotime, Shanghai, China), and the PCR reaction was performed using the ABI 7300 Real-Time PCR equipment (Thermo Fisher Scientific, Waltham, USA). GAPDH served as an internal control, and all samples were run three times. Gene expression was analyzed using the  $2^{-\Delta\Delta CT}$  method [28]. Sequences of primers were listed in [Table S3](#).

### *Western blot analysis and antibodies*

Western blot was used to first determine ANLN protein levels in prostate cancer and normal cell lines, then to determine transfection efficiency after cell transfection, and finally to determine IGF2BP1, c-Myc, and MAPK pathway-related protein expression levels after transfection. The primary antibodies used in the present study are shown in [Table S4](#). After extracting total protein with a Protein Extraction Kit (Beyotime, Shanghai, China) and quantifying protein content with a BSA Protein Quantification Kit (Beyotime, Shanghai, China), the Loading Buffer was added to each sample and cooked at 100°C for 10 minutes. SDS/PAGE gels separated equal quantities of protein, which were then transferred to a PVDF mem-

brane (Millipore, Boston, USA). After blocking for 1.5 hours at room temperature with 5% non-fat milk, membranes were incubated with primary antibodies overnight at 4°C, followed by 1.5 hours at room temperature with secondary antibodies. An improved chemiluminescence detection reagent (Millipore, Boston, USA) was used to detect the signal. As a loading control, GAPDH and  $\alpha$ -tubulin were found.

### *CCK-8 assay*

DU145 and PC-3 cells were seeded in 96-well plates at  $4 \times 10^3$  per well and cultivated for 24 hours for the CCK-8 test. Then, 10  $\mu$ l CCK-8 reagent (Beyotime, Shanghai, China) was added to each well, and absorbance at 450 nm was recorded every 24 hours using a microplate reader (BioTek, USA).

### *EdU assay*

Following the manufacturer's procedure, the BeyoClick EdU Cell Proliferation Kit with Alexa Fluor 555 (Beyotime, Shanghai, China) was used to analyze cell proliferation. The photos were taken with an Olympus IX73 fluorescent inverted microscope system (Olympus, Tokyo, Japan).

### *Clonogenic assay*

Transfected cells were extracted, counted, and planted at a density of 1000 cells/well in 6-well plates for 2 weeks before being fixed with 4% paraformaldehyde for 30 minutes and stained with crystal violet solution for 15 minutes. After that, the colonies were counted and evaluated.

### *Cell cycle measurement*

Cells were collected, fixed with 70% alcohol solution at 4°C for 2 hours, rinsed with ice-cold PBS, then stained for 30 minutes at room temperature with propidium iodide buffer (BD Pharmingen, USA). A Gallios flow cytometer (Beckman Coulter, Brea, USA) was used to measure the cell cycle. The ModFit LT program was used to analyze the results.

### *Transwell assay*

For migration assay, DU145 ( $4 \times 10^4$ /well) and PC-3 ( $8 \times 10^4$ /well), cells were thoroughly resuspended in serum-free media and placed

## Anillin promotes prostate cancer progression

in the upper chambers of transwell plates (Corning, New York City, USA). Simultaneously, the finished medium enriched with 20% FBS was introduced to the Transwell plate's lower chamber. The cells on the bottom surface of the upper chambers were fixed with 4% paraformaldehyde for 30 minutes and stained with crystal violet for 30 minutes after the prescribed culture times (DU145 for 24 hours; PC-3 for 48 hours). Using an inverted microscope (Olympus, Tokyo, Japan), migratory cells were counted in three random visual fields. The bottom surface of the Transwell upper chamber was precoated with diluted matrigel (Corning, New York City, USA) for the invasion test, and the other methods were the same as for the migration experiments.

### Wound-healing assay

The following wound healing tests were carried out. When 90% confluency was obtained, cells were planted on a 6-well plate and scraped with a 200  $\mu$ l pipette tip. Original scratch widths were recorded, then the scratch widths of PC-3 after 24 hours and DU145 after 36 hours were measured. The percentage of wound healing was calculated as the following formula: (original scratch width - scratch width after healing)/ (original scratch width)  $\times$  100%.

### RNA-seq analysis

TRIzol<sup>®</sup> Reagent was used to extract total RNA from DU145 cells transfected with shRNA for ANLN or control shRNA according to the manufacturer's instructions (Magen). RNA samples were detected using a Nanodrop ND-2000 system (Thermo Scientific, USA) and the RIN of RNA was evaluated using an Agilent Bioanalyzer 4150 system (Agilent Technologies, CA, USA). Only qualifying samples will be utilized to build the library. Illumina Novaseq 6000 (Applied Protein Technology Co., Ltd., Shanghai, China) was used to sequence the RNA of DU145 cells transfected with shRNA for ANLN or control shRNA.

### Tumor xenografts in mice

Sixteen 6-week-old BALB/c nude mice were randomly assigned to either the sh-NC or sh-ANLN groups.  $1 \times 10^7$ /mouse DU145 cells (stably transfected with sh-ANLN or sh-NC plasmids) were subcutaneously injected into the

right upper back of the nude mice. The lengths and widths of the tumors were measured once a week by digital calipers, and tumor volumes were calculated using the formula:  $V = (\text{length} \times \text{width}^2)/2$ . All animals were sedated, slaughtered, and the tumors were subsequently removed and gathered for immunohistochemistry (IHC) four weeks later. All laboratory animals were cared for and used in accordance with institutional policies, and they were housed in a pathogen-free environment.

### Gene expression analysis

The ANLN gene expression dataset in prostate cancer was obtained and analyzed from the National Cancer for Biotechnology Information-Gene Expression Omnibus (<https://www.ncbi.nlm.nih.gov/geo/>) and The Cancer Genome Atlas (TCGA) database (<https://www.cancer.gov/ccg/research/genome-sequencing/tcga>).

### Statistical analyses

All experiments were repeated at least three times. Prism 8 (GraphPad Software, San Diego, USA) was used for all statistical analyses. For comparisons, relevant statistical procedures such as Student's t-test, One-way ANOVA, Two-way ANOVA, Wilcoxon matched-pairs signed-rank test, Mann-Whitney U test, and chi-squared test were employed depending on the data type. The significant levels were set at: ns  $P \geq 0.05$ ,  $*P < 0.05$ ,  $**P < 0.01$ ,  $***P < 0.001$  and  $****P < 0.0001$ .

## Results

### *ANLN was highly expressed in prostate cancer and was associated with a poor prognosis*

Previously, we used mRNA microarray analysis to identify a set of differentially expressed mRNAs in 5 matched PCa and ANP tissues [29]. According to this data, ANLN was upregulated in PCa (**Figure 1A**). Besides, we sequenced two pairs of wild-type and highly invasive PC-3 cells and discovered that ANLN was substantially expressed in the highly invasive PC-3 (**Figure S1A**). Using qRT-PCR, we found that ANLN expression was considerably higher in PCa tissues (**Figure 1B** and **1C**). The expression of ANLN was greater in 24 (73.3%) PCa tissues than in corresponding ANP tissues among 30 paired PCa tissues (**Figure S1B**). The mRNA

## Anillin promotes prostate cancer progression

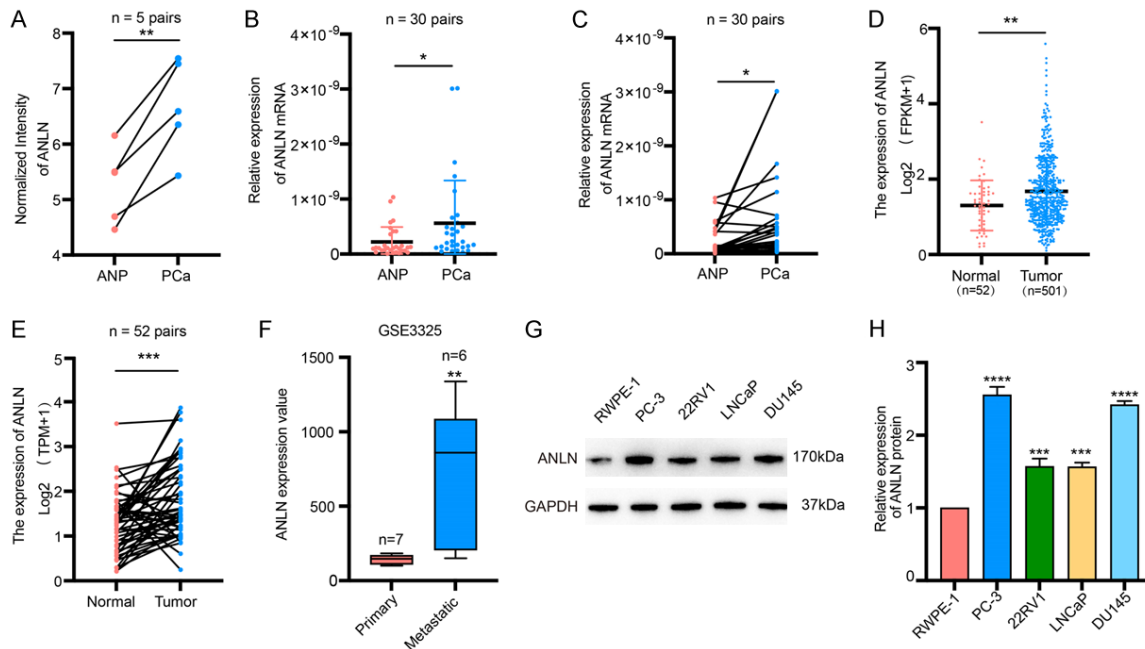


**Figure 1.** ANLN is highly expressed in prostate cancer patients. A. The normalized intensity of ANLN in 5 paired PCa and ANP tissues.  $**P < 0.01$ . B, C. Relative expression of ANLN in ANP and PCa tissues of 30 patients, analyzed by qRT-PCR.  $*P < 0.05$ . D, E. Relative RNA levels of ANLN in prostate cancer and corresponding paraneoplastic tissues in TCGA.  $**P < 0.01$ ,  $***P < 0.001$ . F. Relative RNA levels of ANLN in primary prostate cancer and metastatic prostate cancer in GSE3325.  $**P < 0.01$ . G, H. The ANLN protein expression levels were increased in four prostate cancer cell lines (PC-3, 22RV1, LNCaP and DU145) compared with those in the RWPE-1 cell line.  $***P < 0.001$ ,  $****P < 0.0001$ .

expression profile of ANLN in PCa was then validated using The Cancer Genome Atlas (TCGA) database and the public GEO database. The TCGA dataset revealed that ANLN mRNA expression was increased in PCa compared to normal controls (Figure 1D and 1E). The GSE3325 dataset revealed that ANLN mRNA expression was higher in metastatic prostate cancer than in primary prostate cancer (Figure 1F). ANLN protein levels were measured in PCa cell lines and normal prostate epithelial cells. ANLN was shown to be strongly expressed in PCa cell lines when compared to normal prostate epithelial cells, particularly in DU145 and PC-3 cells (Figure 1G and 1H). The Cancer Genome Atlas (TCGA) database was then used to examine the relationship between ANLN expression and clinical prognosis. We discovered that elevated ANLN expression was associated with advanced T stage, N stage, higher Gleason score, and prostate-specific antigen (PSA) level (Figure 2A-D). ANLN expression and other clinical characteristics in prostate cancer patients were analyzed in Table 1. Patients with greater ANLN expression exhibited a worse prognosis, according to Kaplan-Meier survival curves (Figure 2E and 2F).

### ANLN regulated proliferation in prostate cancer cells

To further explore the biological functions of ANLN in PCa, we first established ANLN knockdown and overexpression systems using si-ANLN and ANLN-copGFP-pLVX-Puro in PC-3 and DU145 cells. After transfection with si-ANLN or ANLN-copGFP-pLVX-Puro, ANLN was drastically downregulated or upregulated, showing that the systems were successfully created. qRT-PCR and Western blot were used to assess the efficacy of knockdown and overexpression (Figure 3A-D). Next, we conducted a series of ANLN cell function experiments. The knocking-down of ANLN dramatically decreased cell proliferation in PC-3 and DU145 cells, according to cell proliferation assays (Figure 3E and 3F), whereas overexpressing ANLN dramatically increased cell proliferation in PC-3 and DU145 cells (Figure 3G and 3H). Similar to this, colony formation experiments showed that colony numbers were significantly reduced when ANLN was silenced and drastically raised when ANLN was overexpressed (Figure 3I-L). This data provides more evidence for the impact of ANLN on PCa cell proliferation. The EdU test consistently

## Anillin promotes prostate cancer progression

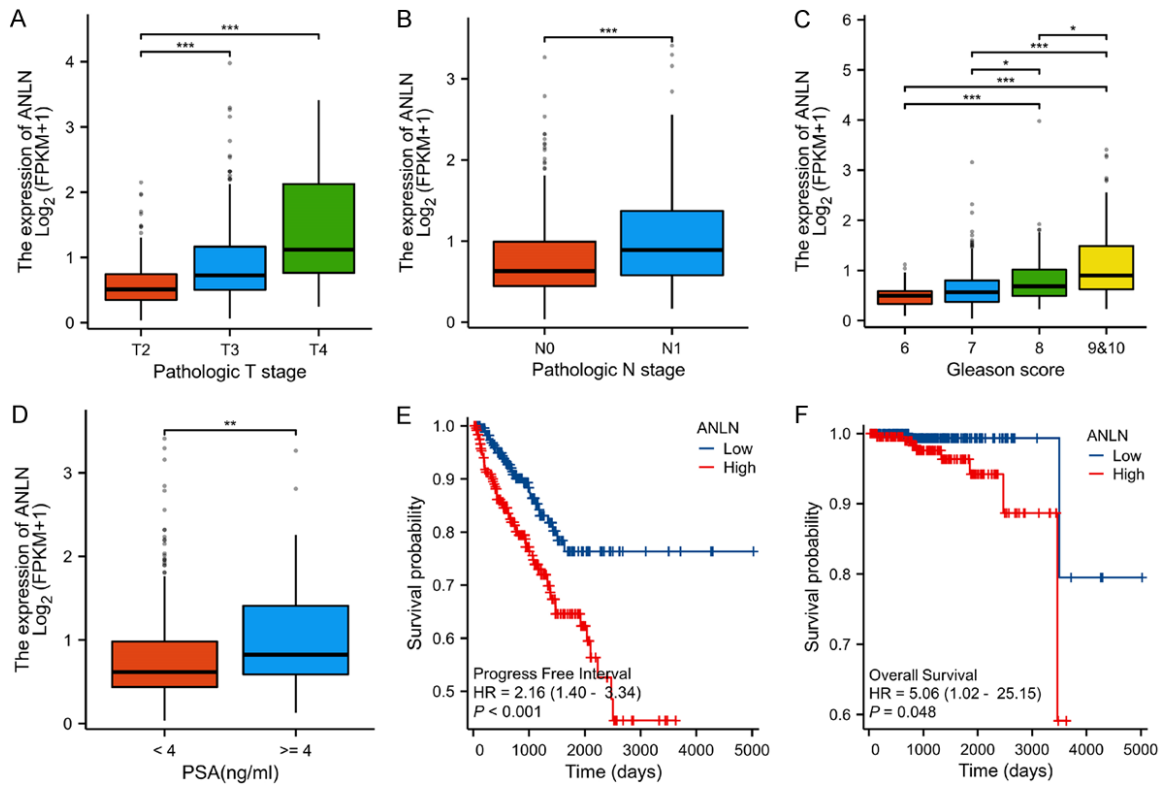


**Figure 2.** ANLN was highly expressed in advanced prostate cancer and was associated with a poor prognosis. A. The correlation between T stage and ANLN expression in prostate cancer. \*\*\* $P < 0.001$ . B. The correlation between N stage and ANLN expression. \*\*\* $P < 0.001$ . C. The correlation between Gleason scores and ANLN expression. \* $P < 0.05$ , \*\*\* $P < 0.001$ . D. The correlation between PSA levels and ANLN expression. \*\* $P < 0.01$ . E. Kaplan Meier curves showed the correlation between ANLN expression and PFI in patients with prostate cancer according to TCGA database. F. Kaplan Meier curves showed the correlation between ANLN expression and OS in patients with prostate cancer according to TCGA database.

confirmed that ANLN downregulation significantly reduced the percentages of EdU-positive cells in PC-3 and DU145 cells, indicating a lower proliferation capacity (Figure 3M and 3N). However, the overexpression of ANLN increased the proportions of EdU-positive cells in PC-3 and DU145 cells, indicating an improved capacity for proliferation (Figure 3O and 3P). Since ANLN dramatically influenced PCa cell proliferation, we next investigated whether knockdown or overexpression of ANLN caused PCa cell proliferation to be inhibited or promoted as a result of arrest in a particular phase of the cell cycle. ANLN deficiency halted the cell cycle at the G1/S junction in PCa cells, according to flow cytometry studies (Figure 4A-D). In contrast, ANLN increase of function accelerate the cell cycle's transition from the G1 to the S phases (Figure 4E-H).

### ANLN inhibits the migration and invasion of PCa cells

We used wound-healing and Transwell assays to more clearly characterize the roles of ANLN

in PCa cell migration and invasion. In wound-healing experiments, ANLN depletion lowered the wound-healing rates of DU145 and PC-3 cells, which was consistent with the proliferation findings (Figure 5A, 5B). However, ANLN overexpression dramatically increased the wound-healing rates (Figure 5C, 5D). Transwell migration and invasion assay findings revealed that, in comparison to the control groups, ANLN knockdown reduced the number of migrating and invading cells (Figure 5E-H). In comparison to the control groups, ANLN overexpression significantly enhanced cell counts for migration and invasion (Figure 5I-L).

### ANLN expression was positively associated with IGF2BP1 expression and MAPK pathways

We performed mRNA-seq on DU145 cells transfected with sh-NC or sh-ANLN to better clarify the molecular mechanisms of ANLN in prostate cancer progression. Sequencing identified 987 genes that were substantially differently expressed, with 169 being upregulated and

## Anillin promotes prostate cancer progression

**Table 1.** Correlation between ANLN expression and clinicopathological characteristics in PCa

Characteristics	Low expression of ANLN	High expression of ANLN	P value
n	250	251	
Pathologic T stage, n (%)			< 0.001
T2	121 (24.5%)	68 (13.8%)	
T3	122 (24.7%)	172 (34.8%)	
T4	3 (0.6%)	8 (1.6%)	
Pathologic N stage, n (%)			0.002
N0	174 (40.7%)	174 (40.7%)	
N1	25 (5.8%)	55 (12.9%)	
Gleason score, n (%)			< 0.001
6	34 (6.8%)	12 (2.4%)	
7	149 (29.7%)	99 (19.8%)	
8	28 (5.6%)	37 (7.4%)	
9&10	39 (7.8%)	103 (20.6%)	
PSA (ng/ml), n (%)			0.026
< 4	216 (48.6%)	201 (45.3%)	
≥ 4	8 (1.8%)	19 (4.3%)	
PFI event, n (%)			< 0.001
No	220 (43.9%)	187 (37.3%)	
Yes	30 (6%)	64 (12.8%)	

Note: The ANLN low and high-expression groups were divided by the median ANLN expression value.

818 being downregulated (**Figure 6A** and **6B**). Furthermore, pathway analysis using data from the Kyoto Encyclopedia of Genes and Genomes (KEGG) revealed that the MAPK signaling pathway was the most significantly enriched (**Figure 6C**). Western blot was used to ascertain if ANLN might impact the expression levels of MAPK related proteins such as p-ERK1/2, p-P38, t-ERK1/2, and t-P38. The expression of ERK1/2 and P38 phosphorylation levels were considerably decreased after ANLN knockdown, but there was no discernible change in total ERK1/2 and P38 expression (**Figure 6D** and **6E**). Overexpression of ANLN could increase phosphorylated ERK1/2 and P38 without altering the total ERK1/2 and P38 (**Figure 6D** and **6E**). We further screened the differential genes as well as experimentally validated them. RT-qPCR and western blotting revealed that IGF2BP1 was significantly downregulated in ANLN-knockdown prostate cancer cells and clearly increased in ANLN-overexpressing cells (**Figures 6D**, **6E** and **S2A-D**). These findings showed that ANLN increased IGF2BP1 expression. IGF2BPs are an RNA-binding protein

(RBP) family with three members (IGF2BP1-3). IGF2BP1 is the most conserved posttranscriptional regulator in the family of IGF2BP proteins, and it is commonly believed to induce pro-oncogenic, pro-proliferative cancer tendencies. However, the study of IGF2BP1 in prostate cancer remains unclear. Therefore, we chose IGF2BP1 for subsequent analyses. Taken together, these data indicated that IGF2BP1 may be a potential downstream target of ANLN. ANLN has the potential to activate the MAPK signaling pathway.

*ANLN promotes prostate cancer progression via IGF2BP1*

We then intended to further elucidate the functions of the ANLN and IGF2BP1 in prostate carcinogenesis by transfection with NC and IGF2BP1-copGFP-pLVX-Puro in ANLN-knockdown PC-3 and DU145 cells. Prostate

cancer cell growth and proliferation were considerably reduced by ANLN knockdown, and these effects were partially reversed by IGF2BP1 transfection (**Figure 6F-J**). Proliferation analysis utilizing EdU assays produced comparable outcomes (**Figures 7A**, **7B**, **S3A** and **S3B**). Moreover, wound-healing assays, transwell migration, and invasion experiments revealed that ANLN knockdown inhibited cell migration and invasion, which were reversed by IGF2BP1 transfection (**Figure 7C-G**). Furthermore, knocking down IGF2BP1 in ANLN overexpression cells will rescue the promoting effect of ANLN overexpression on the proliferation, migration and invasion of prostate cancer cells (**Figures S4** and **S5**).

*ANLN promotes prostate cancer development by stabilizing the proto-oncogene c-Myc and activating the MAPK signaling pathway through IGF2BP1*

As a post-transcriptional regulator, IGF2BP1 affects the transport, translation, and degradation of numerous target mRNAs, including MYC

## Anillin promotes prostate cancer progression

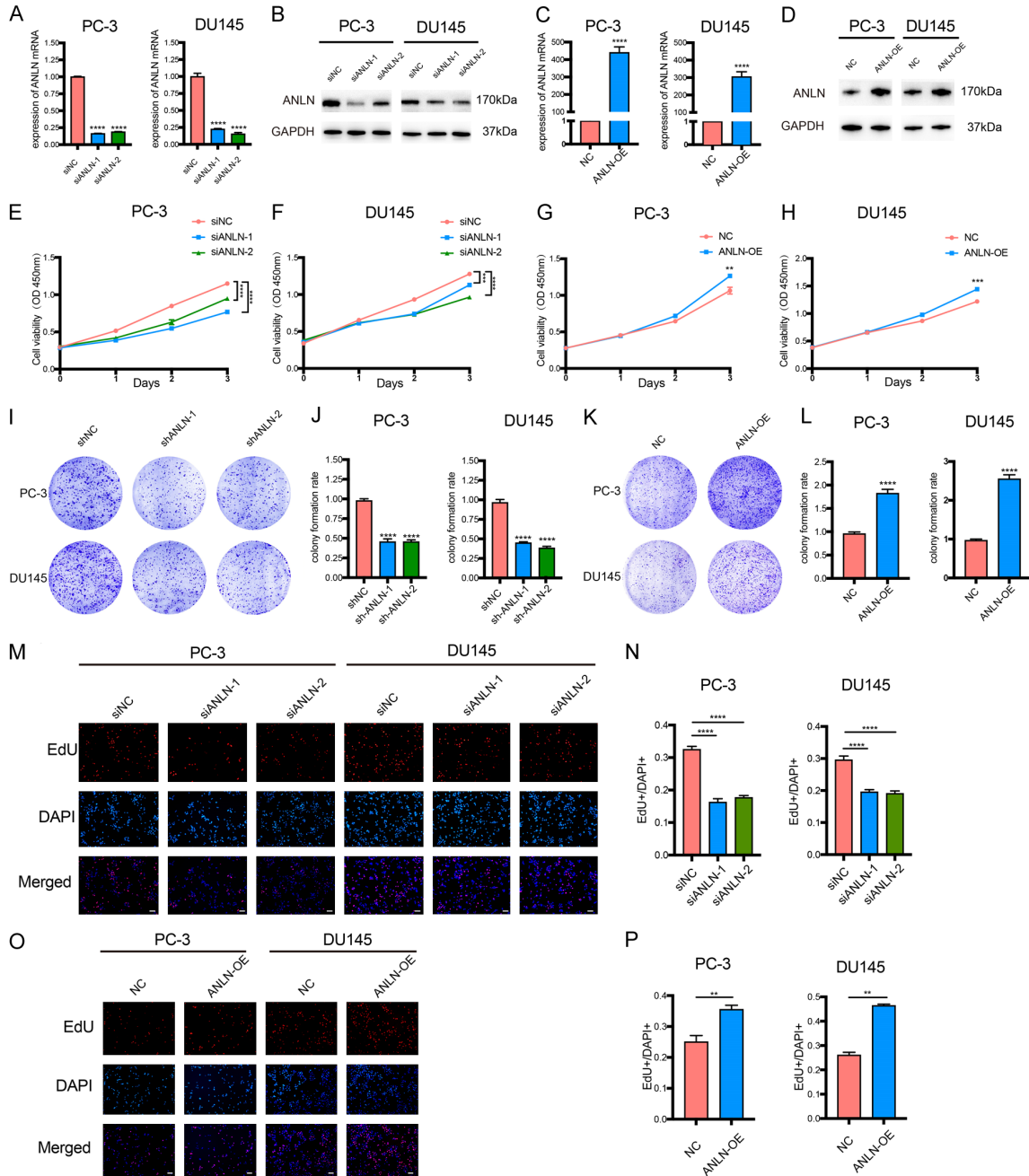


**Figure 3.** ANLN promotes PCa cell proliferation in vitro. A-D. qPCR and western blot analysis showing the knockdown and overexpression efficiency of ANLN.  $****P < 0.0001$ . E-H. Analysis of cell viability in ANLN knockdown and overexpression prostate cancer cells using CCK-8 kit.  $**P < 0.01$ ,  $***P < 0.001$ ,  $****P < 0.0001$ . I-L. Colony formation assay was performed to determine the proliferation of PC-3 and DU145 cells harboring the different vectors indicated.  $****P < 0.0001$ . M-P. Result of EdU assay showing the cell proliferation in ANLN knockdown and overexpression prostate cancer cells.  $**P < 0.01$ ,  $****P < 0.0001$ . Scale bar = 100  $\mu\text{m}$ .

mRNA [15]. IGF2BP1 has been demonstrated to enhance pro-oncogenic powers by sustaining transcription factor expression, which is also crucial for NEN formation and development, by preventing MYC mRNA from being

degraded by endonucleases [30, 31]. It was recently hypothesized that IGF2BP1 regulates MYC mRNA via m6A (N6-methyladenosine) post-transcriptional modification. IGF2BP1 was defined mechanistically as a “m6Areader”, with

# Anillin promotes prostate cancer progression

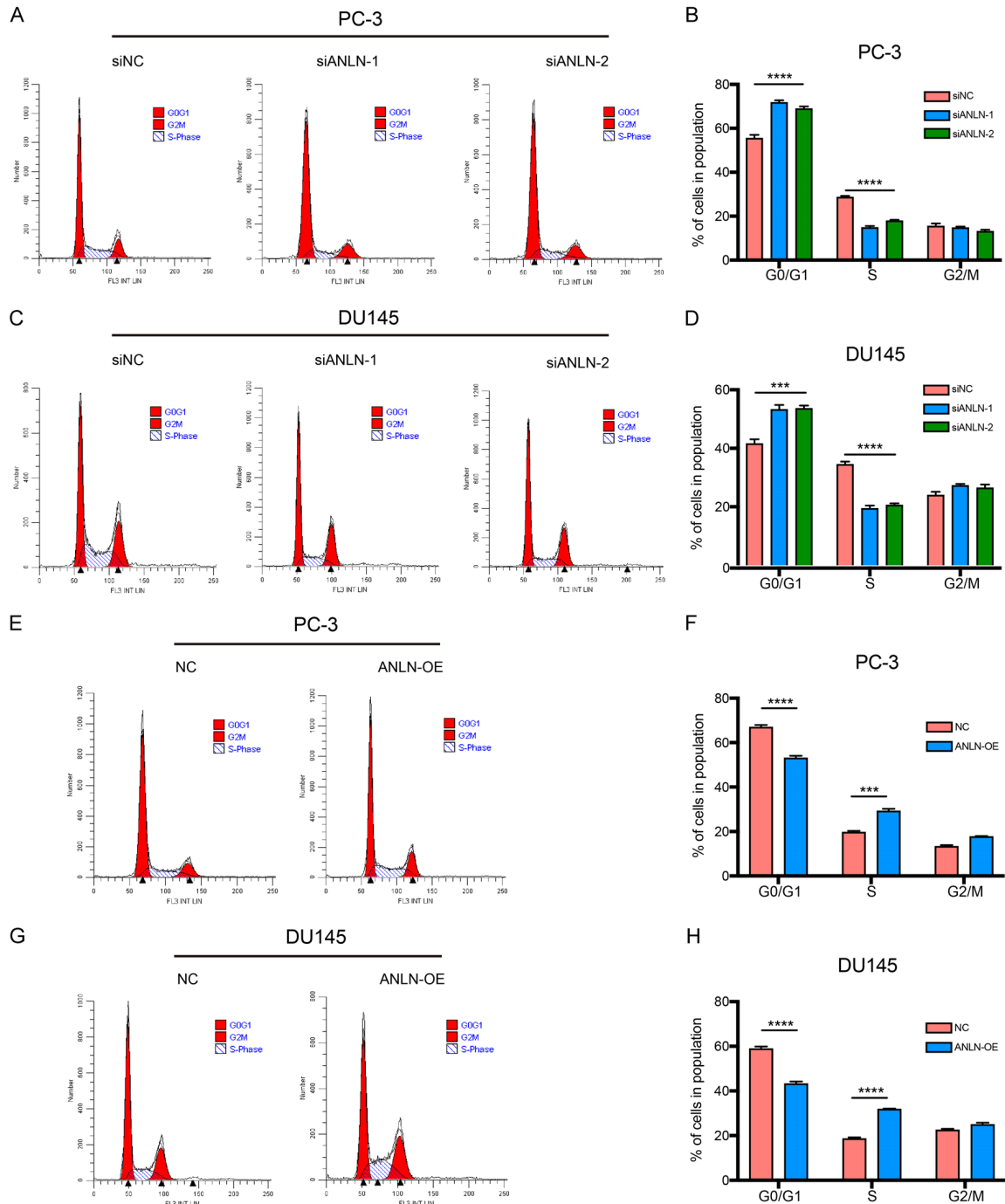


**Figure 4.** ANLN promotes cell cycle progression. A-D. ANLN knock-down increased the percentage of G0/G1 phase and decreased the distribution of S phase in DU145 and PC-3 cells.  $***P < 0.001$ ,  $****P < 0.0001$ . E-H. ANLN-overexpression decreased the percentage of G0/G1 phase and increased the distribution of S phase in DU145 and PC-3 cells.  $***P < 0.001$ ,  $****P < 0.0001$ .

a preference for association with m6A-modified target mRNAs, leading in the protection of target mRNAs from degradation and, as a result, increased protein synthesis [32]. In this research, we found that protein expression of

both IGF2BP1 and c-Myc was reduced after the knockdown of ANLN. However, protein expression of both IGF2BP1 and c-Myc was elevated after overexpression of ANLN (Figure 8A). We next explored whether IGF2BP1 mediates the

# Anillin promotes prostate cancer progression

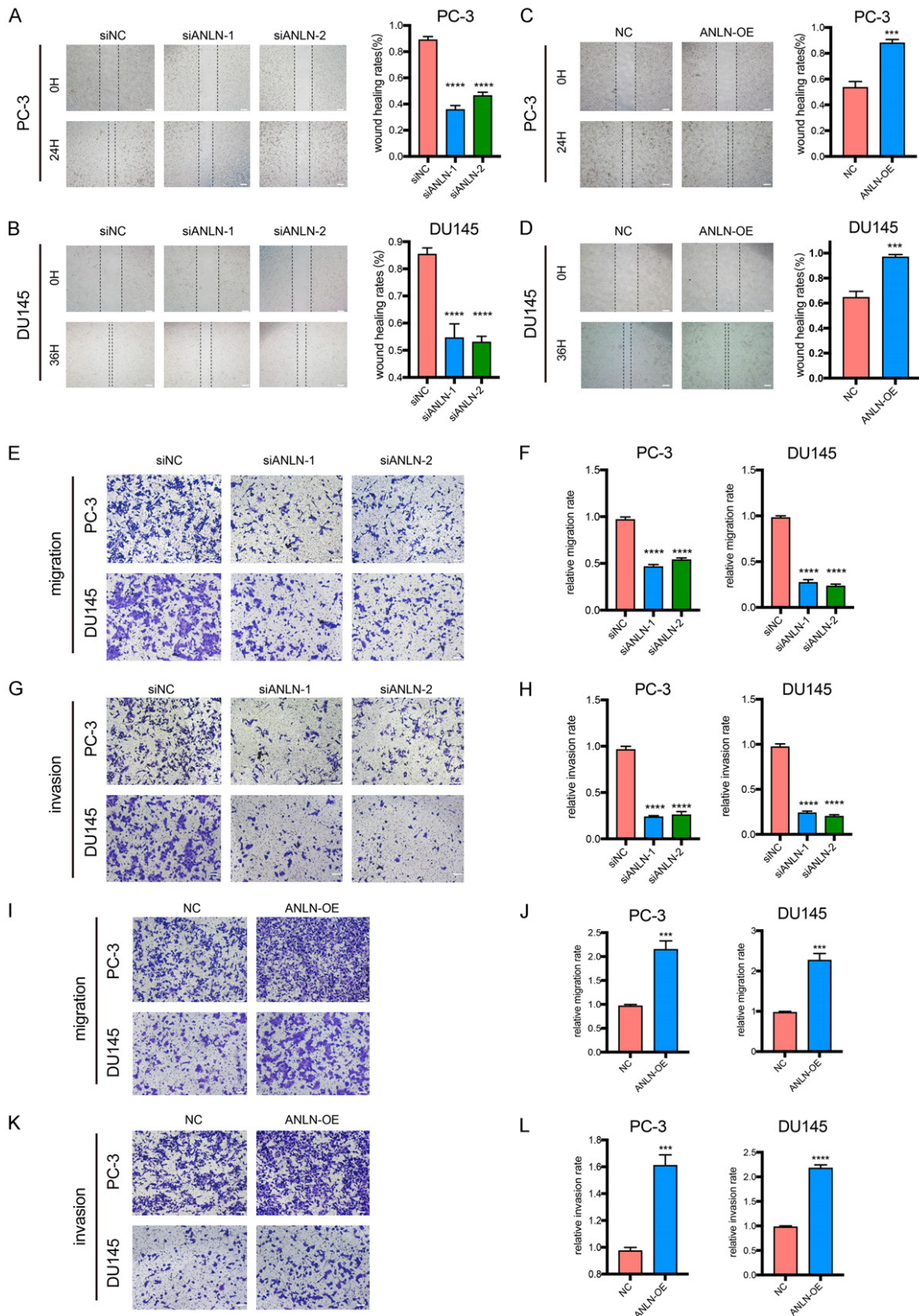


**Figure 5.** ANLN regulated migration, and invasion in prostate cancer cells. A-D. Representative images of the wound-healing assays for prostate cancer cells with ANLN knockdown and overexpression. \*\*\* $P < 0.001$ , \*\*\*\* $P < 0.0001$ . E-H. Cell migration and invasion were assessed with transwell assays in DU145 and PC-3 cells treated with ANLN knockdown. \*\*\*\* $P < 0.0001$ . I-L. Transwell assays were performed to determine the migration and invasion capacity of PC-3 and DU145 cells transfecting with ANLN. \*\*\* $P < 0.001$ , \*\*\*\* $P < 0.0001$ . Scale bar = 100  $\mu\text{m}$ .

# Anillin promotes prostate cancer progression

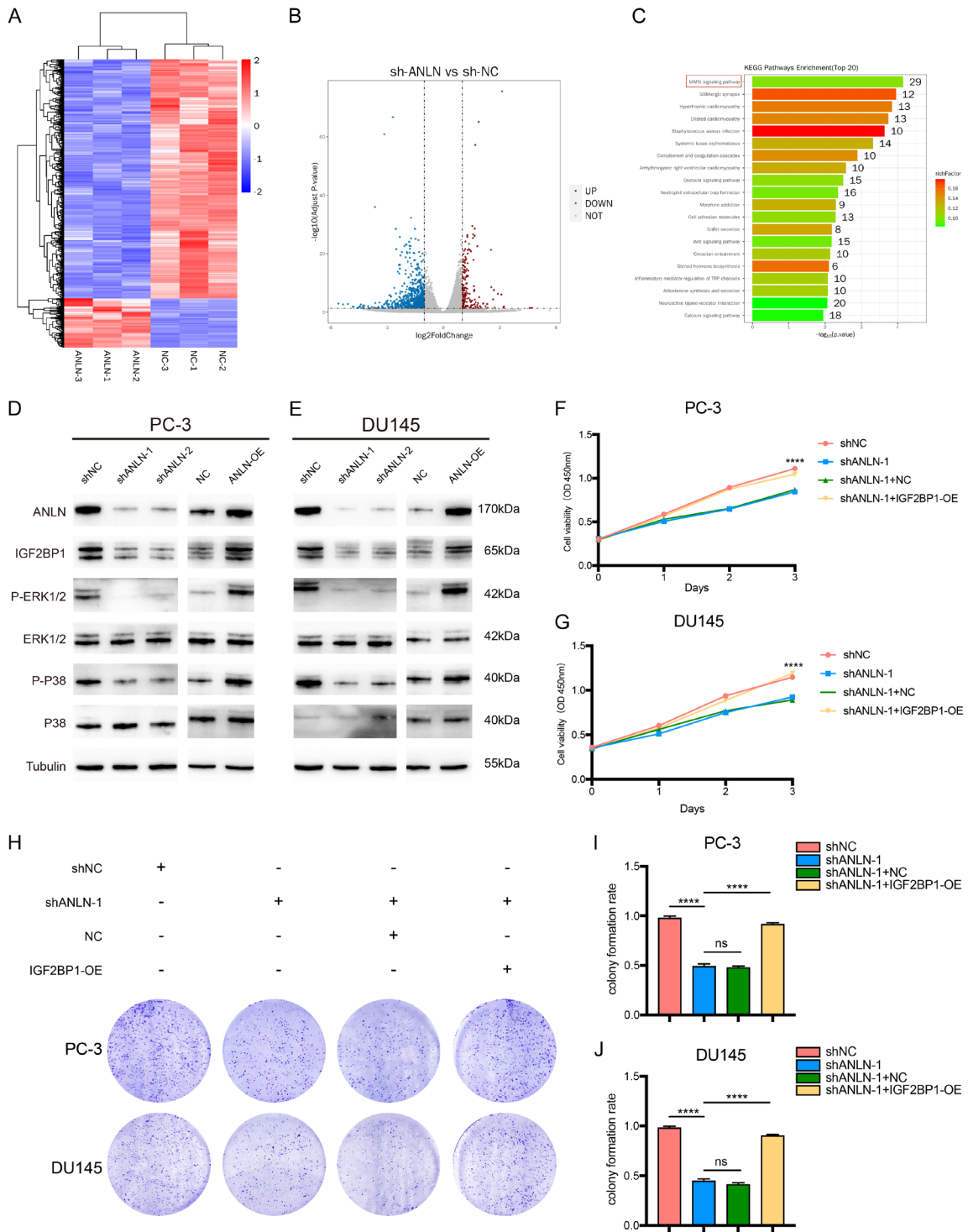


**Figure 6.** ANLN expression was positively correlated with IGF2BP1 expression and MAPK pathways in PCa cells. A. Heatmap illustrating the differentially expressed genes (DEGs) in DU145 cells between shNC group and ANLN knockdown group. B. Volcano map showing the DEGs in DU145 cells between shNC group and shANLN group. C. KEGG pathway analysis of differentially expressed genes based on ANLN-knockdown DU145 cell. D, E. Western blotting analysis of IGF2BP1 and MAPK associated proteins expression in PC-3 and DU145 cells. F, G. Cell mobility was assessed by CCK-8 assays in cells expressing the different constructs. \*\*\*\**P* < 0.0001. H-J. Representative images and quantification of total colonies formed in PC-3 and DU145 cells expressing different vectors. ns *P* ≥ 0.05, \*\*\*\**P* < 0.0001.

# Anillin promotes prostate cancer progression

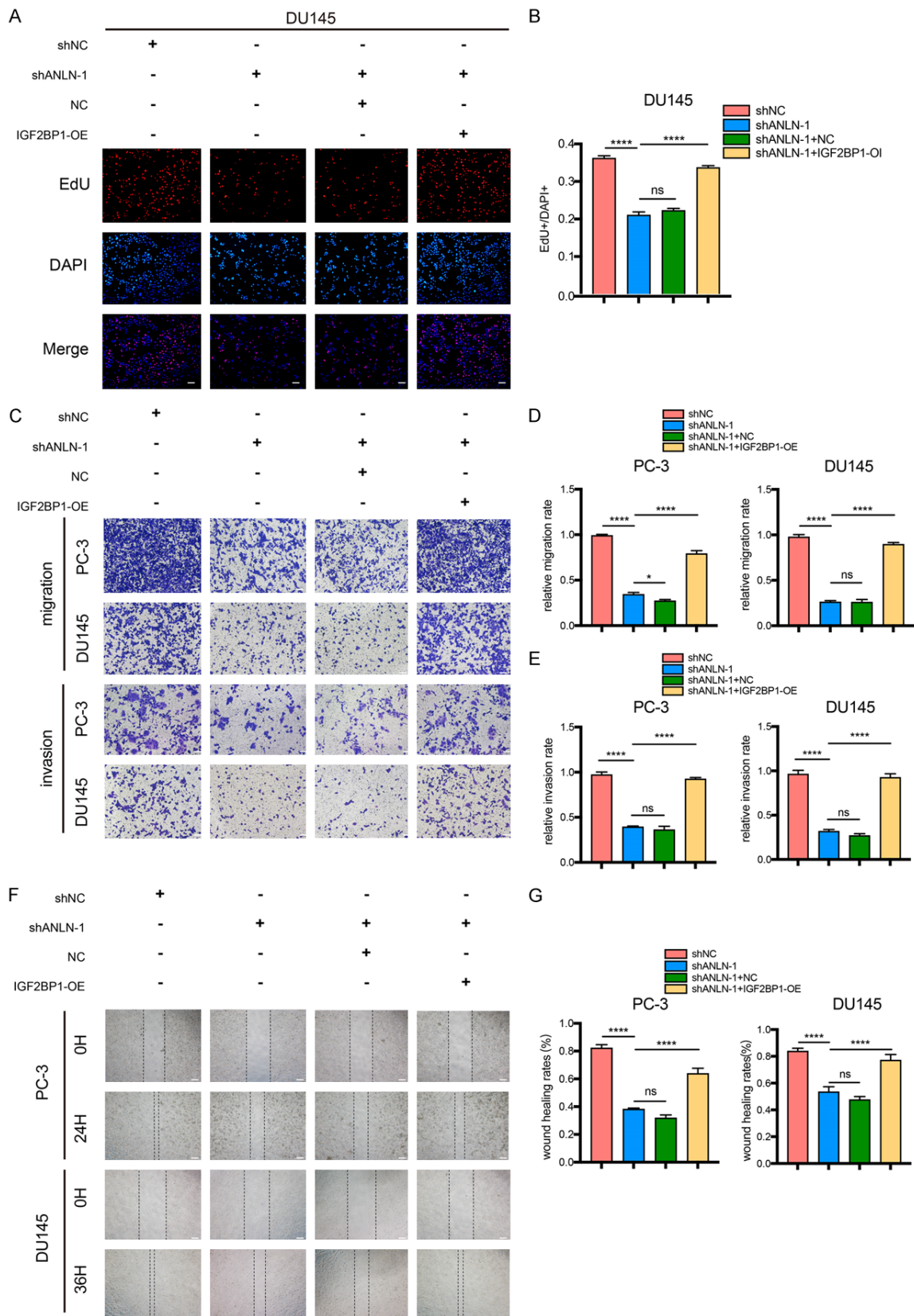


**Figure 7.** ANLN enhances proliferation and metastasis of PCa cells by regulating IGF2BP1. A, B. Result of EdU assay showing the cell proliferation in PC-3 and DU145 cells expressing the different constructs. ns  $P \geq 0.05$ , \*\*\*\* $P < 0.0001$ . C-E. Representative images and quantification of cell migration and invasion in DU145 and PC-3 cells were measured using transwell assays. ns  $P \geq 0.05$ , \* $P < 0.05$ , \*\*\*\* $P < 0.0001$ . F, G. Representative images of the wound-healing assays for prostate cancer cells expressing different vectors. \*\*\*\* $P < 0.0001$ . Scale bar = 100  $\mu\text{m}$ .

# Anillin promotes prostate cancer progression

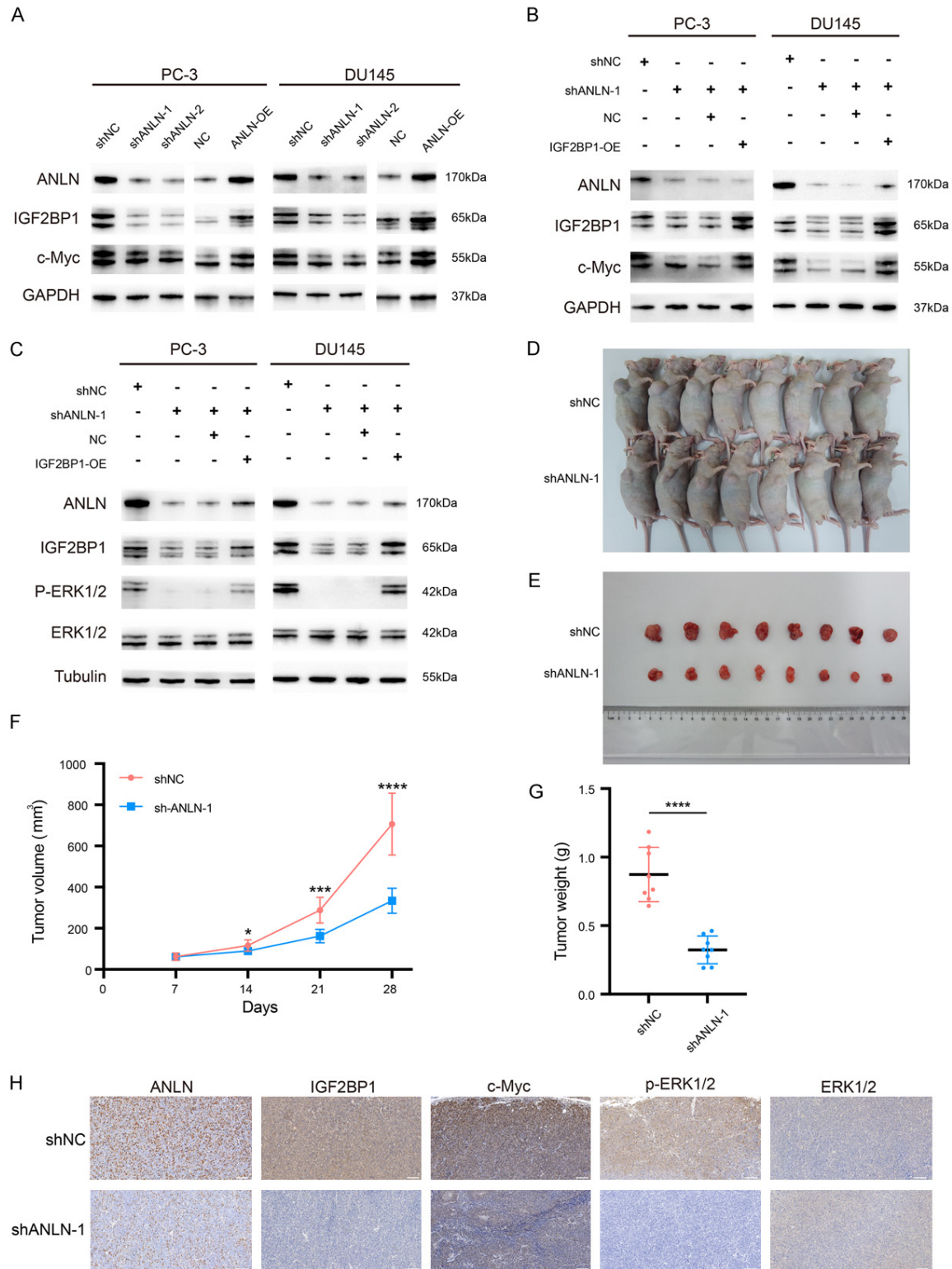


**Figure 8.** ANLN promotes prostate cancer development in vitro and in vivo by stabilizing the proto-oncogene c-Myc and activating the MAPK signaling pathway through IGF2BP1. A. Western blot analysis of IGF2BP1 and c-Myc expression in PC-3 and DU145 cells expressing different vectors. B. Western blot was used to examine the protein expression of c-Myc in cells treated with different vectors. C. Western blot was used to examine the expression of MAPK associated proteins in PC-3 and DU145 cells expressing different vectors. D, E. Xenograft tumor models showed that tumors grown from the shANLN-1 group were smaller than those grown from the shNC group. F, G. The tumor volume changes over time and the tumor weight after dissection.  $***P < 0.001$ ,  $****P < 0.0001$ . H. The representative IHC staining micrographs of ANLN, IGF2BP1 and c-Myc, p-ERK1/2, ERK1/2 in tumor xenografts. Scale bar = 100  $\mu$ m.

regulation of c-Myc by ANLN. Further studies showed that overexpression of IGF2BP1 restored the decrease of c-Myc protein caused by ANLN knockdown (**Figure 8B**). This suggests that ANLN may stabilize the expression of the proto-oncogene c-Myc by regulating IGF2BP1. A previous study reported that IGF2BP1 can regulate the MAPK signaling pathway [33]. Thus, the current work investigated whether ANLN served as an activator of the MAPK signal pathway in PCa by targeting IGF2BP1. After ANLN knockdown, phosphorylated proteins, such as p-ERK1/2, were significantly downregulated in PCa cells, however this result was restored by IGF2BP1 overexpression (**Figure 8C**). Therefore, it was speculated that ANLN activated the MAPK signal pathway by targeting IGF2BP1 in PCa. These results showed that ANLN promoted prostate cancer progression by targeting IGF2BP1 to stabilize the proto-oncogene c-Myc and activate the MAPK signaling pathway.

### *Knockdown of ANLN suppressed prostate tumor growth in vivo*

We successfully created DU145 cells stably expressing shANLN or control cells and injected them into nude mice to further investigate the impact of ANLN on tumor formation in vivo. When compared to the sh-NC group, the sh-ANLN transfectants had a lower tumor formation proportion, tumor growth rate, and tumor weight (**Figure 8D-G**). IHC analysis showed that IGF2BP1, c-Myc, and p-ERK1/2 were expressed at low levels in the ANLN- knockdown group, whereas ERK1/2 was unregulated (**Figure 8H**). Overall, our data revealed that ANLN knockdown prevented prostate carcinogenesis in vivo.

### **Discussion**

Prostate cancer is a common male malignancy with a high mortality rate [34]. The pathophysiological mechanisms that promote the development of prostate cancer remain unclear. Despite the fact that PSA tests have been used for clinical diagnosis for decades, meaningful predictive markers have yet to be discovered. In our previous study [29], we found that ANLN showed a high expression in prostate cancer. Anillin (ANLN) is a Drosophila-derived actin-binding protein that is predominantly identified in cytokinesis [4, 35]. ANLN is recognized as

the primary organizer in the center of the cyto-kinetic machinery because it can draw multiple important cell division-related elements, including F-actin, myosin II, and septins, to the cleavage furrow during cytokinesis [36]. Previous research has demonstrated that ANLN is increased in a range of malignancies and may be used as a potential biomarker for predicting the prognosis of cancer. For instance, it was shown that ANLN expression was enhanced in bladder urothelial carcinoma and that it was linked to a worse prognosis [37]. Consistent with previous findings, our findings demonstrated that ANLN expression was dramatically enhanced in prostate cancer tissues, and cells, and increased ANLN expression was strongly associated with the TNM stage, prostate-specific antigen (PSA) level, and higher Gleason scores in prostate cancer. Moreover, we showed that high ANLN expression was independently associated with a poor prognosis. Furthermore, based on our functional research, we discovered that ANLN was tumorigenic. ANLN knockdown dramatically reduced cell proliferation, migration, and invasion in bladder urothelial cancer, which was consistent with our findings [37]. ANLN knockdown drastically reduced pancreatic cancer cell proliferation, migration, and invasion [13]. Thus, our findings suggest that treatment methods based on ANLN regulation techniques might be a promising strategy for preventing prostate cancer progression.

The mechanism by which ANLN functions in PCa is unknown so far. We utilized RNA-seq to identify candidates of ANLN downstream targets and found IGF2BP1 to be downregulated in prostate cancer cells with ANLN knockdown and there was a positive correlation between ANLN and IGF2BP1 expression in PCa cells. As a m6A reader, IGF2BP1 enhances target mRNA stability and modulates RNA alterations, ultimately contributing to carcinogenesis [38]. IGF2BP1 stabilized c-Myc and MKI67 mRNA in hepatocellular carcinoma (HCC) and elevated serum response factor expression in a m6A-dependent way, promoting HCC development and invasion [38]. In the present study, we found that restoring IGF2BP1 partially reversed the effects of ANLN knockdown on prostate cancer cell proliferation, colony formation, cell migration, and cell invasion. Further research revealed that increased c-Myc might promote tumor progression. Mechanistically, we found that overexpression of IGF2BP1 restored the

## Anillin promotes prostate cancer progression

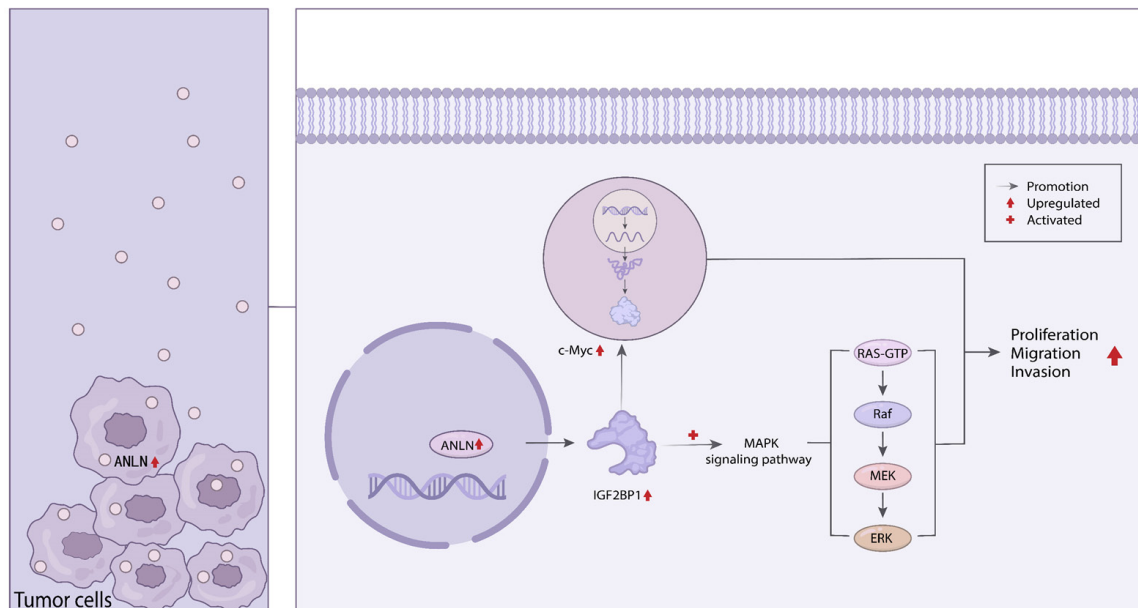


**Figure 9.** Schematic diagram for the role of ANLN in prostate cancer progression. ANLN promotes prostate cancer progression by regulating IGF2BP1 to stabilize the proto-oncogene c-Myc and activate the MAPK signaling pathway.

inhibitory effect of the knockdown of ANLN on c-Myc. These findings showed that ANLN-induced IGF2BP1 overexpression contributes to prostate cancer development.

MAPK signaling pathways play critical roles in translating extracellular inputs into a variety of cellular responses [39]. Three primary MAPKs, ERK, JNK, and p38, are activated at the beginning of many tumor types by mitogens or environmental stress [39]. Despite the complexity of MAPKs' role in the growth of tumors, it is known that they regulate the migration, proliferation, and survival of some cancer cells [39]. The MAPK signal pathway was substantially enriched in the genes with significant enrichment, according to KEGG enrichment analysis of DU145 cells transfected with ANLN shRNA. The MAPK signal pathway is widely recognized for orchestrating widespread tumor characteristics as proliferation, migration, and invasion. MAPK signaling has been shown to be abnormally active in prostate cancer. Still, the specific signaling pathway of ANLN in PCa cells has not been determined. Our present findings revealed that ANLN induced phosphorylation of p38 and ERK1/2 in PCa cell lines, which was prominently inhibited by ANLN knockdown, suggesting that ANLN enhances the phosphorylation of p38 and ERK1/2 MAPKs to activate the MAPK signaling pathway in PCa cells.

Furthermore, IGF2BP1 has been shown to activate the MAPK signaling pathway by inducing ERK phosphorylation, which was verified in the present investigation [40]. Further research revealed that the effects of ANLN knockdown on the MAPK signal pathway were partially reversed by IGF2BP1 restoration. This suggests that ANLN may play a role in promoting prostate cancer progression by regulating IGF2BP1 to activate the MAPK signaling pathway.

In conclusion, our research showed that ANLN overexpression in advanced prostate cancer tissues and cells was correlated with poor outcomes. Furthermore, we discovered that ANLN served as a regulator of cell proliferation, migration, and invasion. Mechanistically, ANLN promotes prostate cancer progression by regulating IGF2BP1 to stabilize the proto-oncogene c-Myc and activate the MAPK signaling pathway (Figure 9). Overall, our findings showed that ANLN might be used as a biomarker for prostate cancer prognosis.

### Acknowledgements

We thanks to everyone who had contributed to this research. This work was supported by grants from the National Science Foundation of Shanghai (grant no. 22ZR1409700 to G.C.), the

## Anillin promotes prostate cancer progression

National Natural Science Foundation of China (grant no. 82303230 to S.W.), the Special Scientific Research Project of Jinshan District Health Commission (grant no. JSKJ-KTMS-2022-05 to S.W.), the Jinshan Hospital Scientific Research Foundation for Young Scholars (grant no. JYQN-JC-202302 to S.W.) and the Project for Key Specialty Construction of Fudan University Jinshan Hospital (grant no. ZDXK-2023-5 to G.C.).

### Disclosure of conflict of interest

None.

**Address correspondence to:** Gang Chen, Department of Urology, Jinshan Hospital, Fudan University, Shanghai 201508, China. E-mail: chen\_gang@fudan.edu.cn; Guoxiong Xu, Research Center for Clinical Medicine, Jinshan Hospital, Fudan University, Shanghai 201508, China. E-mail: guoxiong.xu@fudan.edu.cn; Zhiming Wu, Department of Urology, Sun Yat-sen University Cancer Center, Guangzhou 510060, Guangdong, China. E-mail: wuzhim@susucc.org.cn

### References

- [1] Siegel RL, Miller KD, Wagle NS and Jemal A. Cancer statistics, 2023. *CA Cancer J Clin* 2023; 73: 17-48.
- [2] Teo MY, Rathkopf DE and Kantoff P. Treatment of advanced prostate cancer. *Annu Rev Med* 2019; 70: 479-499.
- [3] Davies A, Conteduca V, Zoubeidi A and Beltran H. Biological evolution of castration-resistant prostate cancer. *Eur Urol Focus* 2019; 5: 147-154.
- [4] Piekny AJ and Maddox AS. The myriad roles of Anillin during cytokinesis. *Semin Cell Dev Biol* 2010; 21: 881-891.
- [5] Tuan NM and Lee CH. Role of Anillin in tumour: from a prognostic biomarker to a novel target. *Cancers (Basel)* 2020; 12: 1600.
- [6] Piekny AJ and Glotzer M. Anillin is a scaffold protein that links RhoA, actin, and myosin during cytokinesis. *Curr Biol* 2008; 18: 30-36.
- [7] Hall PA, Todd CB, Hyland PL, McDade SS, Grabsch H, Dattani M, Hillan KJ and Russell SE. The septin-binding protein anillin is overexpressed in diverse human tumors. *Clin Cancer Res* 2005; 11: 6780-6786.
- [8] Wang Z, Chen J, Zhong MZ, Huang J, Hu YP, Feng DY, Zhou ZJ, Luo X, Liu ZQ, Jiang WZ and Zhou WB. Overexpression of ANLN contributed to poor prognosis of anthracycline-based chemotherapy in breast cancer patients. *Cancer Chemother Pharmacol* 2017; 79: 535-543.
- [9] Schiewek J, Schumacher U, Lange T, Joosse SA, Wikman H, Pantel K, Mikhaylova M, Kneusel M, Linder S, Schmalfeldt B, Oliveira-Ferrer L and Windhorst S. Clinical relevance of cytoskeleton associated proteins for ovarian cancer. *J Cancer Res Clin Oncol* 2018; 144: 2195-2205.
- [10] Wang G, Shen W, Cui L, Chen W, Hu X and Fu J. Overexpression of Anillin (ANLN) is correlated with colorectal cancer progression and poor prognosis. *Cancer Biomark* 2016; 16: 459-465.
- [11] Suzuki C, Daigo Y, Ishikawa N, Kato T, Hayama S, Ito T, Tsuchiya E and Nakamura Y. ANLN plays a critical role in human lung carcinogenesis through the activation of RHOA and by involvement in the phosphoinositide 3-kinase/AKT pathway. *Cancer Res* 2005; 65: 11314-11325.
- [12] Olakowski M, Tyszkiewicz T, Jarzab M, Król R, Oczko-Wojciechowska M, Kowalska M, Kowal M, Gala GM, Kajor M, Lange D, Chmielik E, Gubala E, Lampe P and Jarzab B. NBL1 and anillin (ANLN) genes over-expression in pancreatic carcinoma. *Folia Histochem Cytobiol* 2009; 47: 249-255.
- [13] Wang A, Dai H, Gong Y, Zhang C, Shu J, Luo Y, Jiang Y, Liu W and Bie P. ANLN-induced EZH2 upregulation promotes pancreatic cancer progression by mediating miR-218-5p/LASP1 signaling axis. *J Exp Clin Cancer Res* 2019; 38: 347.
- [14] Wang F, Xiang Z, Huang T, Zhang M and Zhou WB. ANLN directly interacts with RhoA to promote doxorubicin resistance in breast cancer cells. *Cancer Manag Res* 2020; 12: 9725-9734.
- [15] Bell JL, Wächter K, Mühleck B, Pazaitis N, Köhn M, Lederer M and Hüttelmaier S. Insulin-like growth factor 2 mRNA-binding proteins (IGF2BPs): post-transcriptional drivers of cancer progression? *Cell Mol Life Sci* 2013; 70: 2657-2675.
- [16] Jiang X, Liu B, Nie Z, Duan L, Xiong Q, Jin Z, Yang C and Chen Y. The role of m6A modification in the biological functions and diseases. *Signal Transduct Target Ther* 2021; 6: 74.
- [17] Huang X, Zhang H, Guo X, Zhu Z, Cai H and Kong X. Insulin-like growth factor 2 mRNA-binding protein 1 (IGF2BP1) in cancer. *J Hematol Oncol* 2018; 11: 88.
- [18] Dai N, Rapley J, Angel M, Yanik MF, Blower MD and Avruch J. mTOR phosphorylates IMP2 to promote IGF2 mRNA translation by internal ribosomal entry. *Genes Dev* 2011; 25: 1159-1172.
- [19] Nielsen J, Christiansen J, Lykke-Andersen J, Johnsen AH, Wewer UM and Nielsen FC. A fam-

## Anillin promotes prostate cancer progression

- ily of insulin-like growth factor II mRNA-binding proteins represses translation in late development. *Mol Cell Biol* 1999; 19: 1262-1270.
- [20] Suvasini R, Shruti B, Thota B, Shinde SV, Friedmann-Morvinski D, Nawaz Z, Prasanna KV, Thennarasu K, Hegde AS, Arivazhagan A, Chandramouli BA, Santosh V and Somasundaram K. Insulin growth factor-2 binding protein 3 (IGF2BP3) is a glioblastoma-specific marker that activates phosphatidylinositol 3-kinase/mitogen-activated protein kinase (PI3K/MAPK) pathways by modulating IGF-2. *J Biol Chem* 2011; 286: 25882-25890.
- [21] Stöhr N, Köhn M, Lederer M, Glass M, Reinke C, Singer RH and Hüttelmaier S. IGF2BP1 promotes cell migration by regulating MK5 and PTEN signaling. *Genes Dev* 2012; 26: 176-189.
- [22] McCubrey JA, Lahair MM and Franklin RA. Reactive oxygen species-induced activation of the MAP kinase signaling pathways. *Antioxid Redox Signal* 2006; 8: 1775-1789.
- [23] Kholodenko BN and Birtwistle MR. Four-dimensional dynamics of MAPK information processing systems. *Wiley Interdiscip Rev Syst Biol Med* 2009; 1: 28-44.
- [24] Mulholland DJ, Kobayashi N, Ruscetti M, Zhi A, Tran LM, Huang J, Gleave M and Wu H. Pten loss and RAS/MAPK activation cooperate to promote EMT and metastasis initiated from prostate cancer stem/progenitor cells. *Cancer Res* 2012; 72: 1878-1889.
- [25] Fu Z, Smith PC, Zhang L, Rubin MA, Dunn RL, Yao Z and Keller ET. Effects of raf kinase inhibitor protein expression on suppression of prostate cancer metastasis. *J Natl Cancer Inst* 2003; 95: 878-889.
- [26] Clark DE, Errington TM, Smith JA, Frierson HF Jr, Weber MJ and Lannigan DA. The serine/threonine protein kinase, p90 ribosomal S6 kinase, is an important regulator of prostate cancer cell proliferation. *Cancer Res* 2005; 65: 3108-3116.
- [27] Gioeli D, Mandell JW, Petroni GR, Frierson HF Jr and Weber MJ. Activation of mitogen-activated protein kinase associated with prostate cancer progression. *Cancer Res* 1999; 59: 279-284.
- [28] Livak KJ and Schmittgen TD. Analysis of relative gene expression data using real-time quantitative PCR and the 2<sup>-</sup>(Delta Delta C(T)) method. *Methods* 2001; 25: 402-408.
- [29] Song Z, Zhuo Z, Ma Z, Hou C, Chen G and Xu G. Hsa\_Circ\_0001206 is downregulated and inhibits cell proliferation, migration and invasion in prostate cancer. *Artif Cells Nanomed Biotechnol* 2019; 47: 2449-2464.
- [30] Weidensdorfer D, Stöhr N, Baude A, Lederer M, Köhn M, Schierhorn A, Buchmeier S, Wahle E and Hüttelmaier S. Control of c-myc mRNA stability by IGF2BP1-associated cytoplasmic RNPs. *RNA* 2009; 15: 104-115.
- [31] Rickman DS, Schulte JH and Eilers M. The expanding world of N-MYC-driven tumors. *Cancer Discov* 2018; 8: 150-163.
- [32] Huang H, Weng H, Sun W, Qin X, Shi H, Wu H, Zhao BS, Mesquita A, Liu C, Yuan CL, Hu YC, Hüttelmaier S, Skibbe JR, Su R, Deng X, Dong L, Sun M, Li C, Nachtergaele S, Wang Y, Hu C, Ferchen K, Greis KD, Jiang X, Wei M, Qu L, Guan JL, He C, Yang J and Chen J. Recognition of RNA N(6)-methyladenosine by IGF2BP proteins enhances mRNA stability and translation. *Nat Cell Biol* 2018; 20: 285-295.
- [33] Rini J and Anbalagan M. IGF2BP1: a novel binding protein of p38 MAPK. *Mol Cell Biochem* 2017; 435: 133-140.
- [34] Cooperberg MR. Prostate cancer: a new look at prostate cancer treatment complications. *Nat Rev Clin Oncol* 2014; 11: 304-305.
- [35] Field CM and Alberts BM. Anillin, a contractile ring protein that cycles from the nucleus to the cell cortex. *J Cell Biol* 1995; 131: 165-178.
- [36] Hickson GR and O'Farrell PH. Anillin: a pivotal organizer of the cytokinetic machinery. *Biochem Soc Trans* 2008; 36: 439-441.
- [37] Zeng S, Yu X, Ma C, Song R, Zhang Z, Zi X, Chen X, Wang Y, Yu Y, Zhao J, Wei R, Sun Y and Xu C. Transcriptome sequencing identifies ANLN as a promising prognostic biomarker in bladder urothelial carcinoma. *Sci Rep* 2017; 7: 3151.
- [38] Gutschner T, Hämmerle M, Pazaitis N, Bley N, Fiskin E, Uckelmann H, Heim A, Groß M, Hofmann N, Geffers R, Skawran B, Longrich T, Breuhahn K, Schirmacher P, Mühleck B, Hüttelmaier S and Diederichs S. Insulin-like growth factor 2 mRNA-binding protein 1 (IGF2BP1) is an important protumorigenic factor in hepatocellular carcinoma. *Hepatology* 2014; 59: 1900-1911.
- [39] Wagner EF and Nebreda AR. Signal integration by JNK and p38 MAPK pathways in cancer development. *Nat Rev Cancer* 2009; 9: 537-549.
- [40] Zhu Y, Yang L, Wang J, Li Y and Chen Y. SP1-induced lncRNA MCF2L-AS1 promotes cisplatin resistance in ovarian cancer by regulating IGF2BP1/IGF2/MEK/ERK axis. *J Gynecol Oncol* 2022; 33: e75.

## Anillin promotes prostate cancer progression

**Table S1.** The sequences of siRNAs

SiRNAs	Sense (5'-3')	Antisense (5'-3')
si-ANLN-1	UCACAUCUUAUACCACAAATT	UUUGUGGUUUAUGAUGUGAGG
si-ANLN-2	GCCUCUUUGAAUAAAGCCUA	UAGGGCUUUUUAUCAAAGAGGC
si-IGF2BP1	CCAUCCGCAACAUCACAAATT	UUUGUGAUGUUGCGGAUGGTT
si-NC	UUCUCCGAACGUGUCACGU	ACGUGACACGUUCGGAGAA

**Table S2.** The sequences of gene fragments cloned into plasmids

ShRNAs	Sequence (5'-3')
sh-ANLN-1	CCGGCCTCACATCTATAACCACAACTCGAGTTTGTGGTTATAGATGTGAGG TTTTGG
sh-ANLN-2	CCGGGCAAACAAC TAGAAACCAACTCGAGTTGGTTTCTAGTTGTTTGTCTTTTGG
sh-NC	TTCTCCGAACGTGTCACGTCTCGAGACGTGACACGTTCCGAGAATTTTT

**Table S3.** The sequences of primers for qRT-PCR

Primers	Forward (5'-3')	Reverse (5'-3')
ANLN	TGCCAGGCGAGAGAATCTTC	CGCTTAGCATGAGTCATAGACCT
IGF2BP1	GCGGCCAGTTCTTGGTCAA	TTGGGCACCGAATGTTCAATC
$\beta$ -actin	CATGTACGTTGCTATCCAGGC	CTCCTTAATGTCACGCACGAT
GAPDH	GGAGCGAGATCCCTCCAAAAT	GGCTGTTGTCATACTTCTCATGG

**Table S4.** Primary antibodies used in this study

Target	Dilution	Company	Catalog Number
ANLN	1:800	SantaCruz	sc-271814
IGF2BP1	1:5000	Proteintech	22803-1-AP
Total-ERK1/2	1:2000	Proteintech	11257-1-AP
phospho-ERK1/2	1:5000	Proteintech	28733-1-AP
phospho-p38 MAPK	1:1000	Proteintech	28796-1-AP
Total-p38 MAPK	1:1000	Proteintech	14064-1-AP
c-MYC	1:5000	Proteintech	10828-1-AP
GAPDH	1:5000	Proteintech	10494-1-AP
Alpha Tubulin	1:5000	Proteintech	11224-1-AP

## Anillin promotes prostate cancer progression

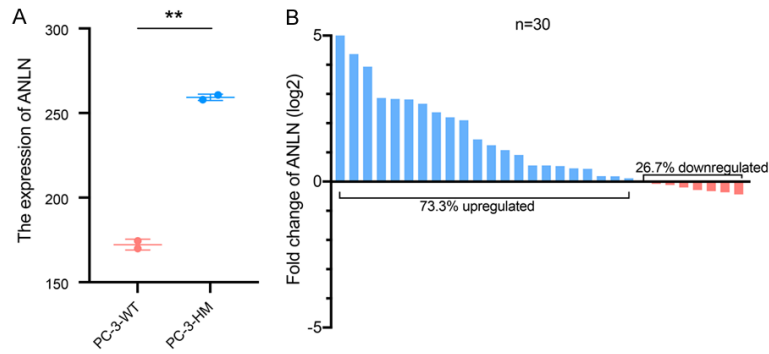


**Figure S1.** A. The normalized intensity of ANLN in two pairs of wild-type and highly invasive PC-3 cells.  $**P < 0.01$ . B. The expression ratio of ANLN in PCa and ANP tissues of 30 patients.

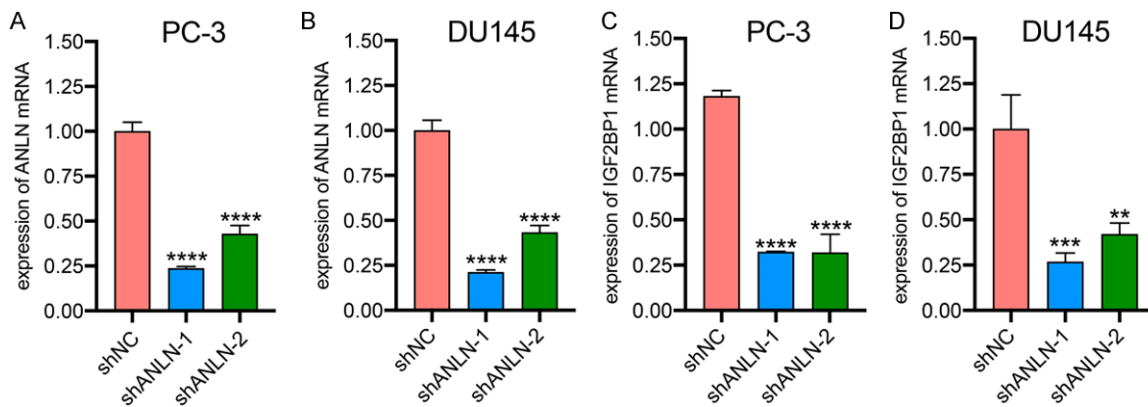


**Figure S2.** A, B. RT-qPCR was used to detect the efficiencies of ANLN knockdown.  $****P < 0.0001$ . C, D. RT-qPCR result showing the expression of IGF2BP1 in PC-3 and DU145 cells treated with ANLN knockdown.  $**P < 0.01$ ,  $***P < 0.001$ ,  $****P < 0.0001$ .

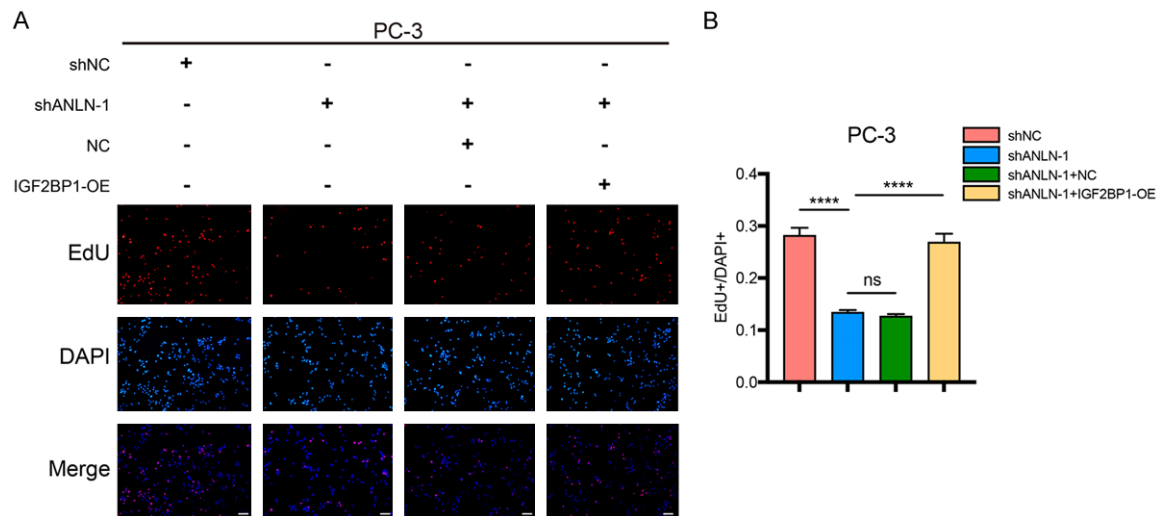


**Figure S3.** A, B. Result of EdU assay showing the cell proliferation in PC-3 cell expressing the different constructs. ns  $P \geq 0.05$ ,  $****P < 0.0001$ . Scale bar = 100  $\mu$ m.

# Anillin promotes prostate cancer progression

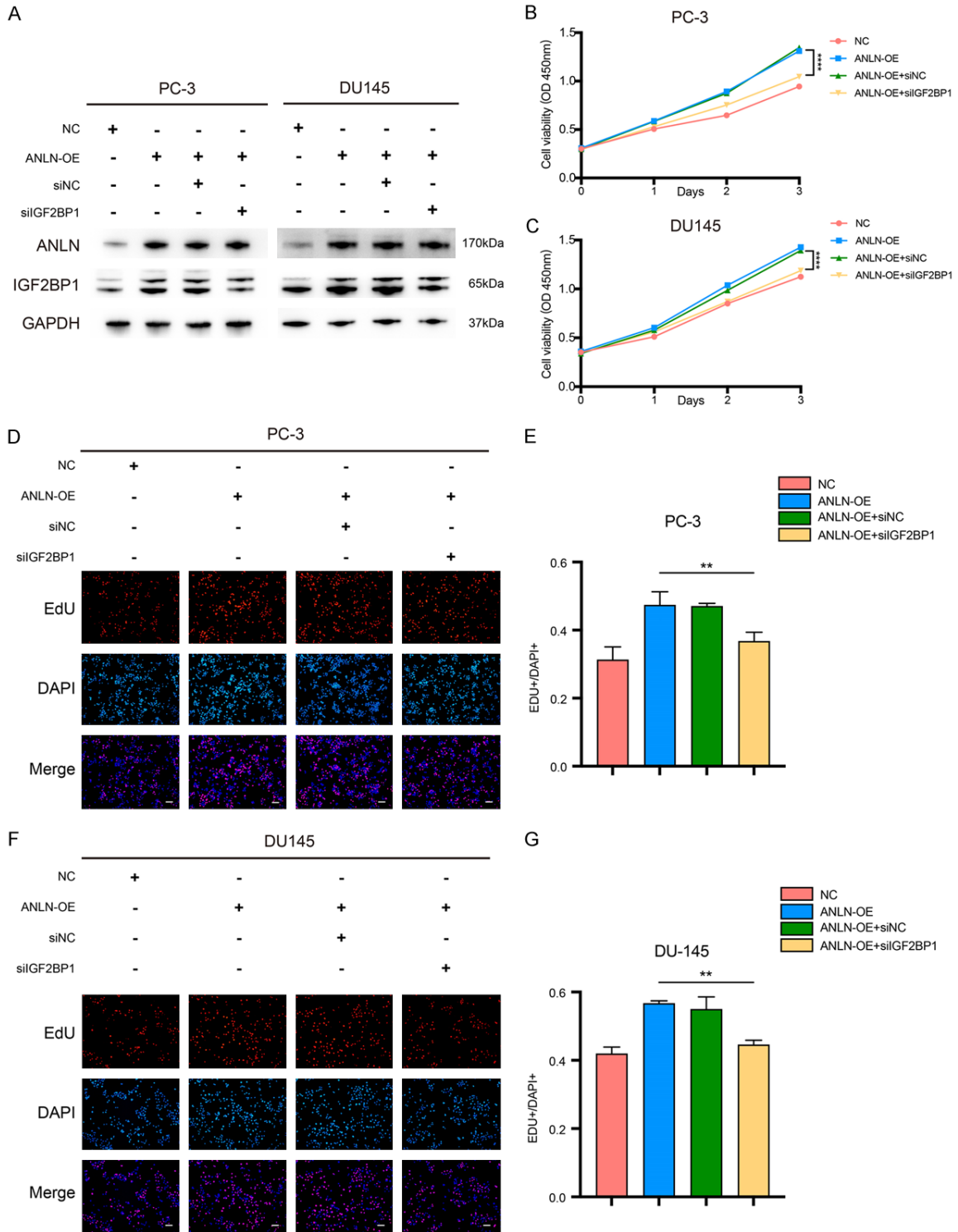


**Figure S4.** Knocking down IGF2BP1 in ANLN overexpression cells will rescue the promoting effect of ANLN overexpression on the proliferation of prostate cancer cells. A. Western blot analysis of ANLN and IGF2BP1 expression in PC-3 and DU145 cells expressing different vectors. B, C. Cell mobility was assessed by CCK-8 assays in cells expressing the different constructs.  $****P < 0.0001$ . D-G. Result of EdU assay showing the cell proliferation in PC-3 and DU145 cells expressing the different constructs.  $**P < 0.01$ . Scale bar = 100  $\mu$ m.

## Anillin promotes prostate cancer progression

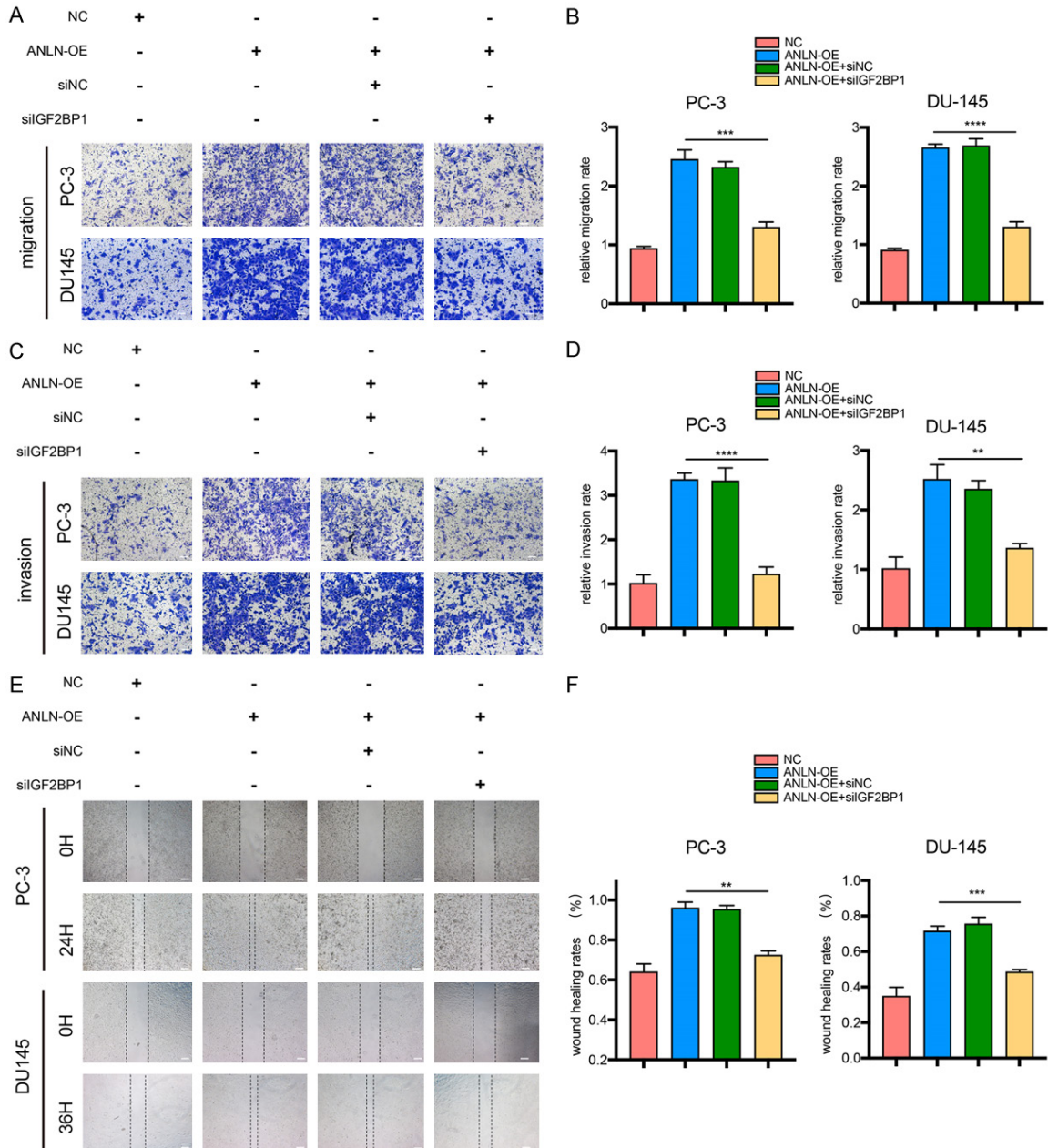


**Figure S5.** Knocking down IGF2BP1 in ANLN overexpression cells will rescue the promoting effect of ANLN overexpression on the migration and invasion of prostate cancer cells. A-D. Representative images and quantification of cell migration and invasion in DU145 and PC-3 cells were measured using transwell assays.  $**P < 0.01$ ,  $***P < 0.001$ ,  $****P < 0.0001$ . E, F. Representative images of the wound-healing assays for prostate cancer cells expressing different vectors.  $**P < 0.01$ ,  $***P < 0.001$ . Scale bar = 100  $\mu\text{m}$ .